Separation Science and Technology
Publication details, including instructions for authors and subscription information:
http://www.informaworld.com/smpp/title~content=t713708471

Reactor Analysis of an Electrochemical Caustic Concentrator

N. R. K. Vilambi[a]; E. J. Taylor[a]; R. Waterhouse[a]; A. Gelb[a]
[a] PSI TECHNOLOGY COMPANY, ANDOVER, MASSACHUSETTS

To cite this Article Vilambi, N. R. K. , Taylor, E. J. , Waterhouse, R. and Gelb, A.(1990) 'Reactor Analysis of an Electrochemical Caustic Concentrator', Separation Science and Technology, 25: 5, 627 — 652
To link to this Article: DOI: 10.1080/01496399008050354
URL: http://dx.doi.org/10.1080/01496399008050354

SEPARATION SCIENCE AND TECHNOLOGY, 25(5), pp. 627-652, 1990

Reactor Analysis of an Electrochemical Caustic Concentrator

N. R. K. VILAMBI, E. J. TAYLOR, R. WATERHOUSE, and A. GELB

PSI TECHNOLOGY COMPANY
20 NEW ENGLAND BUSINESS CENTER
ANDOVER, MASSACHUSETTS 01810

Abstract

Physical Sciences Inc. is developing an electrochemical caustic concentrator (ECC) to reduce the energy requirements of a membrane chloralkali plant. The ECC is a membrane alkaline fuel cell which consumes the by-product hydrogen from the chloralkali cell and oxygen from air to generate dc power and concentrate the caustic soda in the cathode compartment. We are developing a process development unit (PDU) of the ECC in order to verify its operating characteristics. As part of this effort, we developed a detailed reactor model of the PDU. In this model we use data from our gas diffusion electrode and membrane development studies. Our analysis indicates that with state-of-the-art components, the caustic soda from the chloralkali cell can be concentrated to 50 wt% with the generation of dc electricity.

INTRODUCTION

The chloralkali industry is one of the major industrial electrochemical industries and produces chlorine, sodium hydroxide, and by-product hydrogen. In the United States this industry consumes energy equivalent to 287,000 barrels of oil daily (*1, 2*). Any improvement in the energy efficiency of the chloralkali process would have a significant effect on United States energy consumption.

Physical Sciences Inc. (PSI) developed and patented (*3*) a unique process with the potential of reducing the energy consumption of a membrane chloralkali process up to a maximum of 30% (*4*). One of the energy-intensive unit operations in the membrane chloralkali process is the con-

concentration of the reactor effluent stream (to reduce shipping costs) from 30 to 50 wt% by using thermal evaporators. In the PSI process the conventional evaporators are replaced with the electrochemical caustic concentrator (ECC). The ECC is an alkaline fuel cell with a membrane separator. It consumes the by-product hydrogen from the chloralkali cell and oxygen from air to concentrate caustic and also simultaneously produces dc power. In the past few years, considerable research efforts have been focused on developing and characterizing porous gas diffusion electrodes (*5*) and membranes (*6*) for the ECC environment. Currently work is in progress to integrate the individual components of the ECC in a process development unit (PDU) to experimentally verify and optimize the operating parameters for the PSI process.

This paper is concerned with a reactor analysis study of the PDU of the ECC. The objective of developing the model for the PDU is to help understand the role of the various transport processes and their relative effects on the performance of the ECC. A parametric study on the caustic concentration distribution in the cathode and anode compartments and the corresponding cell voltages were computed. The parameters investigated include: 1) electrode polarization, 2) membrane transport properties, 3) membrane conductivity, 4) electrolyte flow rates, 5) electrolyte temperature, 6) gas flow rates, 7) gas temperature, 8) gas humidity, and 9) current density.

REACTOR ANALYSIS

Figure 1 shows the schematic of the ECC. It consists of four compartments: 1) anode gas compartment, 2) anode electrolyte compartment, 3) cathode electrolyte compartment, and 4) cathode gas compartment. Porous gas diffusion electrodes separate the gas and electrolyte compartments. A cation-exchange membrane separates the two electrolyte compartments. Caustic from the electrolysis cell (30 wt%) is fed into the anode and cathode electrolyte compartments. Oxygen gas (or air) and hydrogen gas are passed through the cathode and anode gas compartments, respectively. Oxygen and water react at the cathode to produce hydroxyl ions, whereas hydrogen and hydroxyl ions react at the anode to produce water. The cation-exchange membrane permits the transport of sodium ions and water from the anode to cathode compartments. The net process involves continuous addition of sodium hydroxide and removal of water from the catholyte stream, thereby affecting concentration of the feed catholyte stream. Conversely, the anolyte stream is diluted.

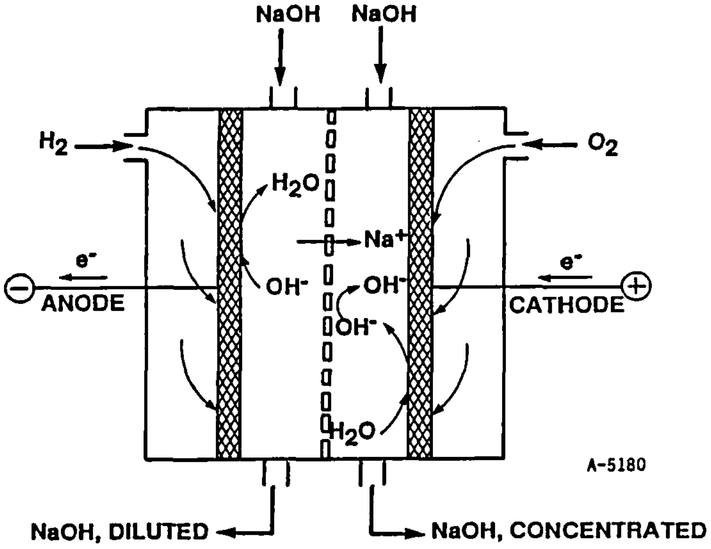

FIG. 1. Schematic of ECC.

To simplify the analysis, the following assumptions were made: (i) coflow scheme exists, i.e., the anolyte and catholyte streams flow in the same direction; (ii) plug flow conditions exist in the anode and cathode electrolyte compartments, (iii) the anode and cathode gas compartments are well mixed; (iv) current distribution at the electrodes is uniform; (v) there are isothermal reactor conditions; (vi) there is steady-state operation; (vii) there is parallel plate cell configuration; and (viii) the outlet gas streams are saturated with water vapor. The plug flow conditions in the electrolyte compartments imply that no mixing is permitted in the axial direction whereas perfect mixing is permitted in the transverse direction. Consequently, the concentration varies only in the axial direction.

With these assumptions the ECC resembles a sandwich of: (a) continuously stirred tank reactor, CSTR, (anode gas compartment); (b) plug flow reactor, PFR, (anode electrolyte compartment); (c) plug flow reactor, PFR, (cathode electrolyte compartment); and (d) continuously stirred tank reactor, CSTR, (cathode gas compartment). The two PFR's are interconnected with the ion-exchange membrane whereas each CSTR is connected to the PFR with the electrode. Figure 2 shows a schematic of the ECC and the flow streams associated with each compartment. The reactor

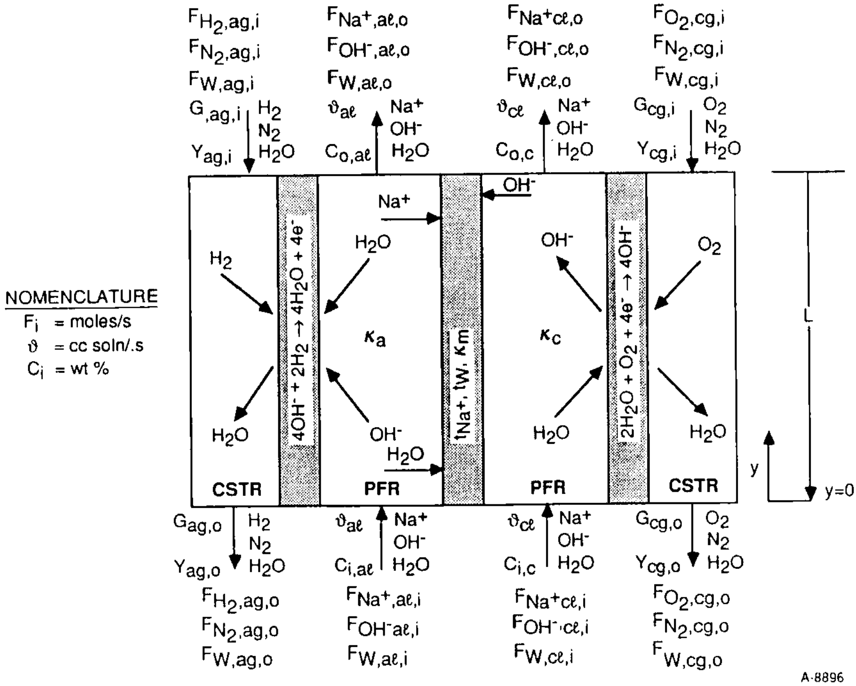

FIG. 2. Schematic of flow streams and flow conditions in the ECC.

analysis of the ECC to simulate its concentrating ability and its cell voltage characteristics now reduce to solving the material balance and voltage balance equations for the system of reactors and the flow conditions as shown in Fig. 2.

MATERIAL BALANCE

A material balance is done for each individual cell compartment. As mentioned above, the two electrolyte compartments are treated as two PFR's whereas the two gas compartments are treated as two CSTR's.

The overall electrochemical reaction in the cell is

$$2H_2 + O_2 \rightarrow 2H_2O \tag{1}$$

The partial reactions occurring at the cathode and the anode are

$$O_2 + 2H_2O + 4e^- \rightarrow 4OH^- \tag{2}$$

$$2H_2 + 4OH^- \rightarrow 4H_2O + 4e^- \tag{3}$$

In setting up the material balance, the following notation was followed: R denotes rate of production, F denotes molar flow rate, subscript w denotes water, subscript Na^+ denotes sodium ion, subscript OH^- denotes hydroxyl ions, subscript N denotes sodium hydroxide, subscript H_2 denotes hydrogen, subscript O_2 denotes oxygen, subscript i denotes inlet, subscript o denotes outlet, subscript a denotes anode, subscript c denotes cathode, subscript al denotes anode electrolyte compartment, subscript cl denotes cathode electrolyte compartment, subscript ag denotes anode gas compartment, and subscript cg denotes cathode gas compartment. The species considered for material balance were water, hydrogen, oxygen, and sodium ion. Further, the law of electroneutrality gives

$$F_{\mathrm{Na}^+} = F_{\mathrm{OH}^-} = F_{\mathrm{NaOH}} \tag{4}$$

A. Anode Gas Compartment

Since the anode gas compartment is a CSTR, the steady-state material balance for water and hydrogen is given by

Water

$$F_{w,ag,i} + F_{w,a} = F_{w,ag,o} \tag{5}$$

$$F_{w,ag,i} = G_{ag,i} Y_{ag,i} \tag{6}$$

$$F_{w,ag,o} = G_{ag,o} Y_{ag,o} \tag{7}$$

where $F_{w,a}$ is the total molar rate of water transport through the anode into the gas phase, G is the molar flow rate of dry gas, and Y is the molal absolute humidity.

Hydrogen

$$F_{H_2,aq,i} + R_{H_2,a} = F_{H_2,aq,o} \tag{8}$$

$$R_{H_2,a} = \frac{-[2isL]}{4F} \tag{9}$$

where i is the current density, s is the surface area of the electrode per length of the reactor, L is the length of the reactor, and F is Faraday's constant. Note that the rate of hydrogen production, $R_{H_2,a}$, is negative that is, hydrogen is consumed at the anode.

B. Anode Electrolyte Compartment

The anode electrolyte compartment is a PFR with varying electrolyte concentration along its length. Since the membrane properties vary as a function of electrolyte concentration, the molar flux of water and sodium ion varies as a function of the axial distance, denoted by y. Setting up a differential mass balance, the differential equations describing the molar flux of water and sodium ion in the anode electrolyte compartment are given by

Water

$$\frac{dF_{w,al}}{dy} = \frac{-[ist_{Na^+}\tau_w]}{F} + \frac{[is]}{F} - \frac{F_{w,a}}{L} \tag{10}$$

The first term represents water transported across the membrane, the second term represents water produced at the anode, and the last term represents the molar flow rate of water through the anode into the anode gas chamber.

Sodium Ion

$$\frac{dF_{Na^+,al}}{dy} = - \frac{[ist_{Na^+}]}{F} \tag{11}$$

where t_{Na^+} is the sodium ion transport number and τ_w is the relative water transport number of the membrane. The relative water transport number for the membrane is defined as the ratio of the water transport number to the sodium transport number. As mentioned above, the transport properties of the membrane are functions of the NaOH concentrations in the anolyte and catholyte compartments and hence vary along the length of the reactor.

C. Cathode Electrolyte Compartment

Similar to the anode electrolyte compartment, setting up a differential mass balance in the catholyte chamber, the differential equations describing the molar flux of water and sodium ion in the cathode electrolyte compartment are given by

Water

$$\frac{dF_{w,cl}}{dy} = \frac{[ist_{Na^+}\tau_w]}{F} - \frac{[is]}{2F} - \frac{F_{w,c}}{L} \tag{12}$$

The first term represents the water transport across the membrane, the second term represents water consumption at the cathode, and the third term is the molar flow rate of water transport through the cathode into the gas phase.

Sodium Ion

$$\frac{d_{Na^+,cl}}{dy} = \frac{[ist_{Na^+}]}{F} \tag{13}$$

D. Cathode Gas Compartment

Similar to the anode gas compartment, the steady-state material balance for water and oxygen is given by

Water

$$F_{w,cg,i} + F_{w,c} = F_{w,cg,o} \tag{14}$$

$$F_{w,cg,i} = G_{cg,i}Y_{cg,i} \tag{15}$$

$$F_{w,cg,o} = G_{cg,o}Y_{cg,o} \tag{16}$$

where $F_{w,c}$ is the total rate of water transport through the cathode into the gas phase, G is the molar flow rate of dry gas, and Y is the molar absolute humidity.

Oxygen

$$F_{O_2,cg,i} + R_{O_2,c} = F_{O_2,cg,o} \tag{17}$$

$$R_{O_2,a} = -\frac{[isL]}{4F} \tag{18}$$

Equations (4) to (18) completely describe the individual component material balance for the ECC and must be solved simultaneously to determine the water and NaOH molar concentration profiles in each compartment. The concentration of the caustic in weight percent can then be calculated as

$$C_N = \frac{[F_{Na^+}M_N] \times 100}{[F_{Na^+}M_N + F_w M_w]} \tag{19}$$

where M denotes molecular weight.

VOLTAGE BALANCE

The voltage loss in the cell is due to polarization loss at the anode, ohmic loss in the anolyte, ohmic loss across the membrane, ohmic loss in the catholyte, and polarization loss at the cathode. Thus the voltage balance is given by

$$E_{cell} = E_o + \eta_c - \eta_a - [IR]_a - [IR]_c - [IR]_m \tag{20}$$

$$[IR]_a = \frac{[it_a]}{k_a} \tag{21}$$

$$[IR]_c = \frac{[it_c]}{k_c} \tag{22}$$

$$[IR]_m = \frac{[it_m]}{k_m} \tag{23}$$

where E_{cell} is the cell voltage, E_o is the open circuit cell voltage, subscript m denotes membrane, η is the total electrode overpotential, $[IR]_a$ is the ohmic loss in the anode electrolyte compartment, $[IR]_c$ is the ohmic loss in the cathode electrolyte compartment, $[IR]_m$ is the voltage drop across the membrane, t is thickness, and k is the electrical specific conductivity. The specific conductivity of the electrolyte and the membrane are strong functions of the caustic concentration. Hence Eqs. (20) to (23) must be solved together with the material balance equations to calculate the cell voltage.

INPUT DATA

To solve the material balance and voltage balance equations, several input data are required regarding the properties of the electrode, membrane, and electrolyte in the ECC environment as a function of the anolyte and catholyte concentrations. The input data required for the ECC simulations are: 1) membrane transport properties, 2) membrane conductivity, 3) electrolyte conductivity, 4) electrode polarization behavior, 5) vapor pressure of water, and 6) electrolyte density.

1. Transport Properties of Membrane

The water transport and sodium transport numbers determine the amount of sodium ion and molecular water transported through the membrane from the anolyte side to the catholyte side. Experimental measurements of the sodium ion transport and water transport numbers were made at 75°C over a matrix of anolyte and catholyte caustic concentrations for different membranes (*6*). In Figs. 3 and 4 we present the data for a proprietary membrane supplied by Du Pont. The sodium and water transport numbers are strong functions of the anolyte and catholyte concentrations. The values obtained from the experimental measurements mentioned above were used in the calculations.

2. Electrical Conductivity of Membrane

The electrical conductivity of the membrane determines the voltage loss across the membrane. The conductivity of the membranes investigated were experimentally measured at 75°C over a matrix of anolyte and

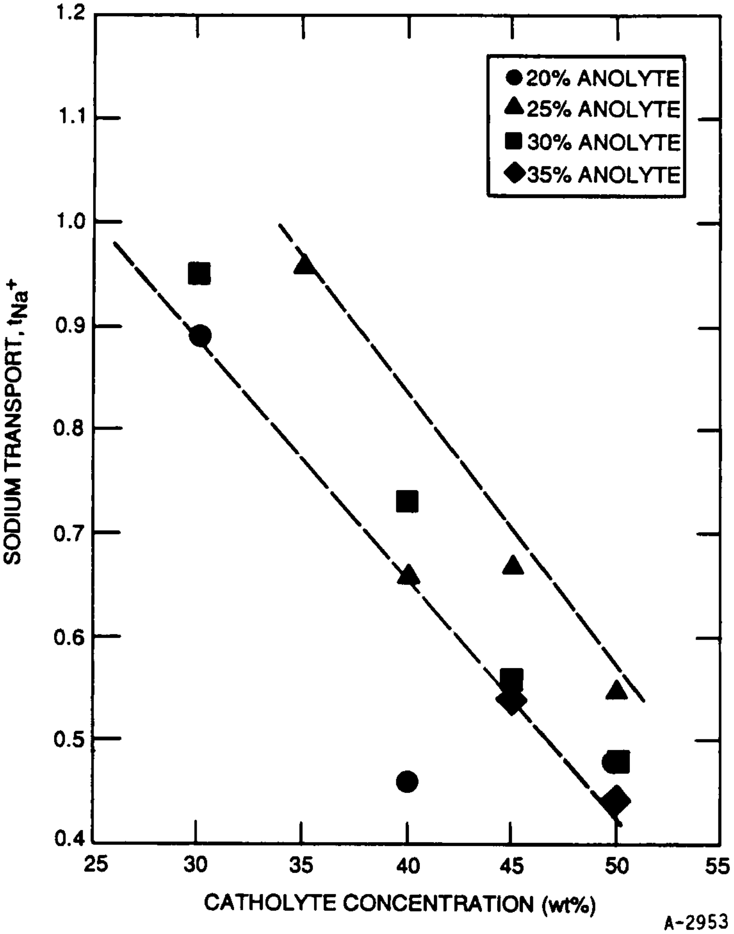

FIG. 3. Sodium transport data for Du Pont's proprietary membrane A-1.

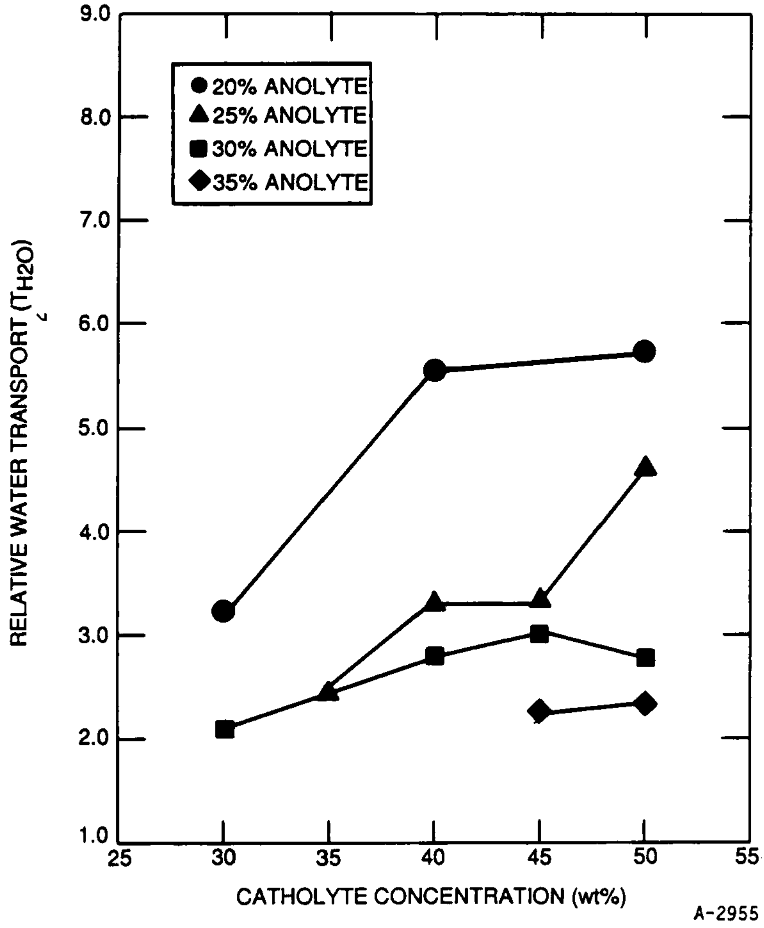

FIG. 4. Water transport data for Du Pont's proprietary membrane A-1.

catholyte caustic concentrations (*6*). The conductivity of the membrane is also a strong function of the current density, and the concentrations of the caustic on the anolyte and the catholyte side of the membrane (see Fig. 5). The values obtained from the experimental measurements mentioned above were used in the calculations.

3. Electrical Conductivity of Electrolyte

The ohmic loss in the anolyte and catholyte is determined by the electrical conductivity of the electrolyte and cell gap. Experimental measurements of the electrical conductivity of NaOH were made over a range of caustic concentrations and temperatures (*7*) of interest to the ECC. The electrical conductivity of NaOH decreased with increasing concentrations and decreasing temperatures. The values obtained from the experimental measurements mentioned above were used in the calculations.

4. Electrode Polarization Behavior

The polarization losses suffered at the electrodes directly influence the cell voltage delivered by the ECC. The porous gas diffusion electrodes are made of high-surface-area carbon, small platinum particles, and Teflon. The type of carbon used, size of platinum particles, platinum loading, Teflon content, electrode thickness, and sintering temperature affect the performance of these electrodes. An experimental study on the effect of these different parameters on the performance (polarization behavior) of these electrodes was conducted (*5*). Optimum cathode performance was obtained with an electrode made of Ketjen Black EC300J carbon (>850 m^2/g), 10% platinum loading (<15 Å platinum particles), 30% Teflon, and 300°C sintering temperature. The anode performance data were obtained with an electrode made of Vulcan XC-72 carbon (>250 m^2/g), 10% platinum loading (<15 Å platinum particles), 50% Teflon, and 325°C sintering temperature. The anode and cathode polarization data are shown in Fig. 6 and were used in the calculations.

5. Vapor Pressure Data

In order to compute the amount of water vapor carried away by the gas streams, vapor pressure data for water are required for any given temperature. These data were obtained from Ref. *8*.

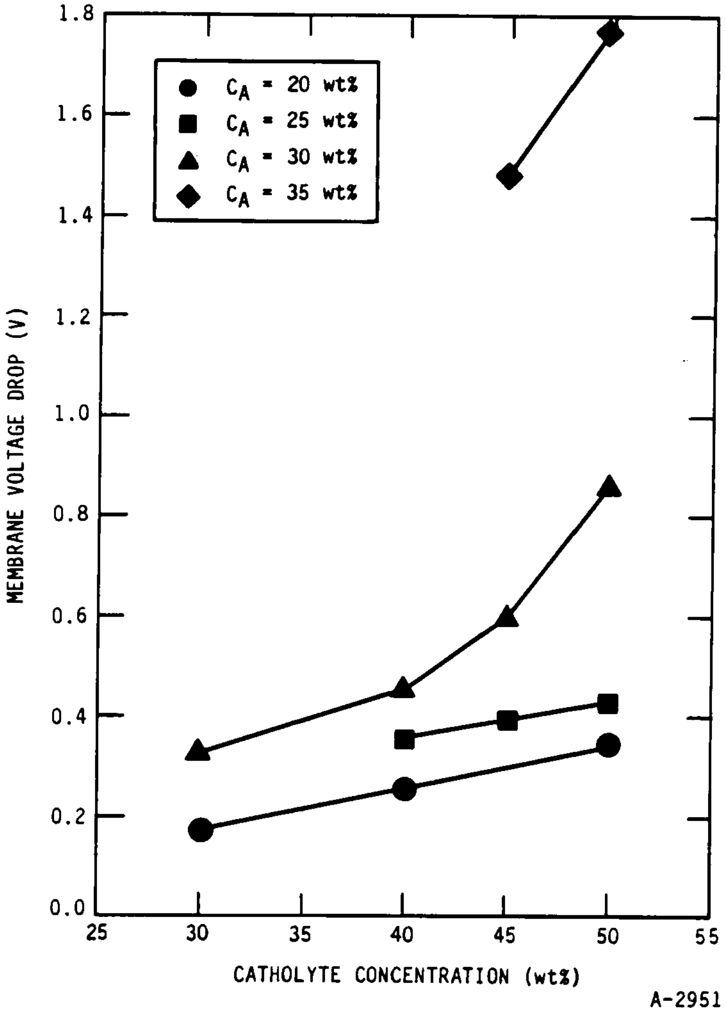

FIG. 5. Voltage drop data for Du Pont's proprietary membrane A-1 at a current density of 100 mA/cm^2.

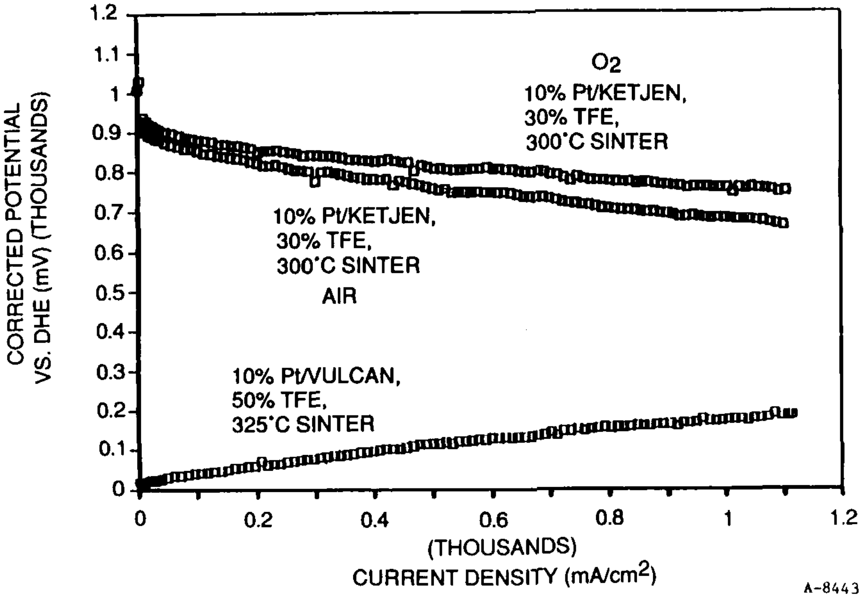

FIG. 6. Anode and cathode polarization data.

6. Density of Sodium Hydroxide

In order to calculate the individual molar flow rates of NaOH and water for a given volumetric flow rate and wt% caustic, the density of sodium hydroxide is required as a function of the concentration of sodium hydroxide in wt% for any given electrolyte temperature. These data were obtained from Ref. 9.

INPUT PARAMETERS

The main input parameters for the problem are: 1) current density, 2) surface area of electrode per unit length of the reactor, 3) length of the reactor, 4) oxygen utilization, 5) hydrogen utilization, 6) electrolyte temperature, 7) inlet gas temperature, 8) outlet gas temperature, 9) anolyte feed concentration, 10) catholyte feed concentration, 11) anode compartment thickness, 12) cathode compartment thickness, 13) volumetric flow rate of catholyte, 14) volumetric flow rate of anolyte, and 15) the type of membrane used.

SOLUTION TECHNIQUE AND PROCEDURE

Equations (4) through (23) represent a system of coupled nonlinear algebraic and differential equations describing the material balance and the voltage balance in the ECC. The differential equations were converted into algebraic equations by discretization using a forward difference scheme.

Anolyte Water Balance

$$\frac{F_{w,al(y_{i+1})} - F_{w,al(y_i)}}{y_{i+1} - y_i} = \frac{-[ist_{\mathrm{Na}^+(y_i)} t_{w(y_i)}]}{F} + \frac{[is]}{F} - \frac{F_{w,a}}{L} \tag{24}$$

Anolyte Sodium Ion Balance

$$\frac{F_{\mathrm{Na}^+,al(y_{i+1})} - F_{\mathrm{Na}^+,al(y_i)}}{y_{i+1} - y_i} = \frac{-[ist_{\mathrm{Na}^+(y_i)}]}{F} \tag{25}$$

Catholyte Water Balance

$$\frac{F_{w,cl(y_{i+1})} - F_{w,cl(y_i)}}{y_{i+1} - y_i} = \frac{[ist_{\mathrm{Na}^+(y_i)} \tau_{w(y_i)}]}{F} - \frac{[is]}{2F} - \frac{F_{w,c}}{L} \tag{26}$$

Catholyte Sodium Ion Balance

$$\frac{F_{\mathrm{Na}^+,cl(y_{i+1})} - F_{\mathrm{Na}^+,cl(y_i)}}{y_{i+1} - y_i} = \frac{[ist_{\mathrm{Na}^+(y_i)}]}{F} \tag{27}$$

The initial conditions are given by the feed specifications to the anolyte and catholyte compartments. The entire reactor was then discretized into differential elements of thickness Δy. For a given set of input parameters, the anolyte and catholyte concentration profiles and the cell voltages were computed by solving Eqs. (4)-(9) and (14)-(27) for each differential element beginning at $y = 0$ and marching through the length of the reactor in increments of Δy. The entire procedure was repeated with decreasing Δy until convergence was attained. A computer code in Fortran has been developed on a VAX minicomputer to solve the above problem and is available on request.

RESULTS AND DISCUSSION

The values of the input parameters used in this simulation study for the ECC PDU are given in Table 1. These values were chosen based on the following criteria: 1) availability of transport data for membranes, 2) availability of conductivity data for membranes, 3) availability of electrode polarization data for the anode and the cathode, 4) availability of hydrogen corresponding to feed caustic from the chloralkali cell, and 5) practical alkaline fuel cell operating data.

The parameters investigated include: 1) catholyte flow rate, 2) anolyte flow rate, and 3) different cation-exchange membranes. The cell temperature was set at 75°C. The inlet gas streams were assumed to be saturated at room temperature and the exit streams to be saturated at the cell temperature.

In Fig. 7(a) and 7(b) we present the effect of the catholyte flow rate on the sodium hydroxide concentration profiles in the catholyte and anolyte compartments. The membrane chosen for analysis is an advanced devel-

TABLE 1
Values of Input Parameters for the ECC PDU Model

Parameters	Value	Units
Current density, i	0.10	A/cm^2
Surface area per unit length, s	5.0	cm^2/cm
Reactor length, L	150	cm
Oxygen utilization	20	%
Hydrogen utilization	80	%
Cathode gas feed	Air	
Electrolyte temperature	75	°C
Gas inlet temperature	25	°C
Gas outlet temperature	75	°C
Anolyte feed concentration	30	wt%
Catholyte feed concentration	30	wt%
Anode compartment thickness	50	mils
Cathode compartment thickness	50	mils

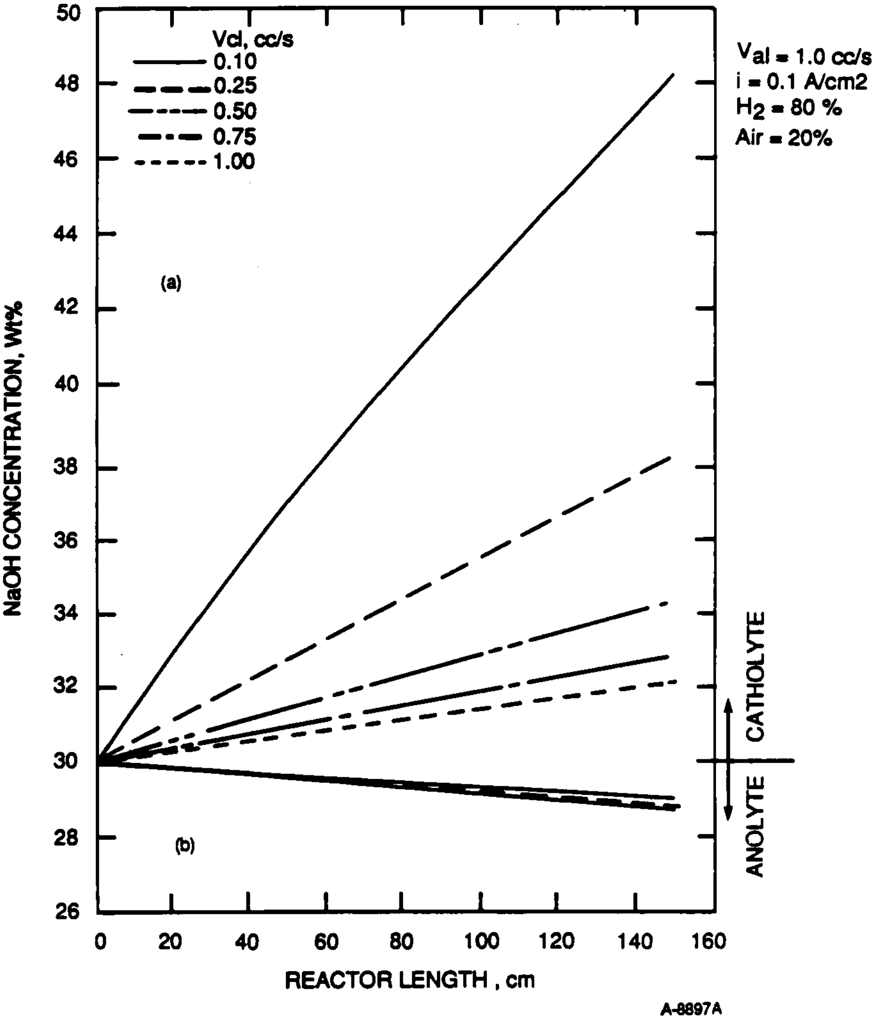

FIG. 7. Effect of catholyte flow rate on (a) catholyte concentration profile and (b) anolyte concentration profile in the ECC.

opmental membrane by Du Pont designated A-1. The catholyte flow rates were varied from 0.1 to 1.0 cm^3/s, and the anolyte flow rate was held constant at 1.0 cm^3/s. The length of the reactor was fixed based on the current density in the ECC and the availability of hydrogen corresponding to the minimum catholyte flow rate. In general, the catholyte concentration increases with increasing length of the reactor (see Fig. 7a). With a catholyte flow rate of 0.1 cm^3/s, the exit concentration is close to 50 wt%. However, with increasing catholyte flow rates, the exit catholyte concentration decreases considerably. Another interesting feature is that as the catholyte flow rate decreases, the catholyte concentration profile becomes nonlinear. This results from the changing membrane transport properties due to varying anolyte and catholyte concentrations along the length of the reactor. In general, as the catholyte concentration is increased, the sodium transport number decreases and the water transport number increases. The anolyte concentration decreased with increasing length of the reactor (see Fig. 7b). The catholyte flow rate did not significantly influence the anolyte concentration profiles. This is primarily due to the fact that the anolyte flow rate is always significantly higher than the catholyte flow rates. As the catholyte flow rate approaches the anolyte flow rate, the dilution of the anolyte stream relative to the catholyte stream increases.

The effect of the catholyte flow rate on the ECC cell voltage is shown in Fig. 8. The cell voltage initially increased noticeably as the catholyte flow rate was increased from 0.1 to 0.25 cm^3/s and remained relatively unchanged for higher catholyte flow rates. The lower cell voltages observed at lower flow rates are due to increased membrane and electrolyte resistances as the catholyte concentration increases.

To better understand the effect of the anolyte flow rate on the performance of the ECC, a set of computer simulations was run with the catholyte flow rate fixed at 0.1 cm^3/s and varying the anolyte flow rate from 0.1 to 1.0 cm^3/s. The results of these computer simulations are presented in Figs. 9 and 10. The catholyte concentration profile remained relatively unchanged for anolyte flow rates of 0.25 to 1.0 cm^3/s (see Fig. 9a). However, with an anolyte flow rate of 0.1 cm^3/s, the exit catholyte concentration decreases noticeably. The corresponding anolyte concentration profiles are given in Fig. 9(b). The anolyte flow rate had a significant effect on the anolyte concentration profiles. With decreasing anolyte flow rates the exit anolyte stream became more and more diluted and the anolyte concentration profile became more nonlinear. This is again due to the nonlinear relationship between the transport properties of the membrane and the anolyte/catholyte concentrations. In general, as the anolyte concentration decreases, the water transport number increases. This results in a decrease in the catholyte exit concentration at low anolyte flow rates.

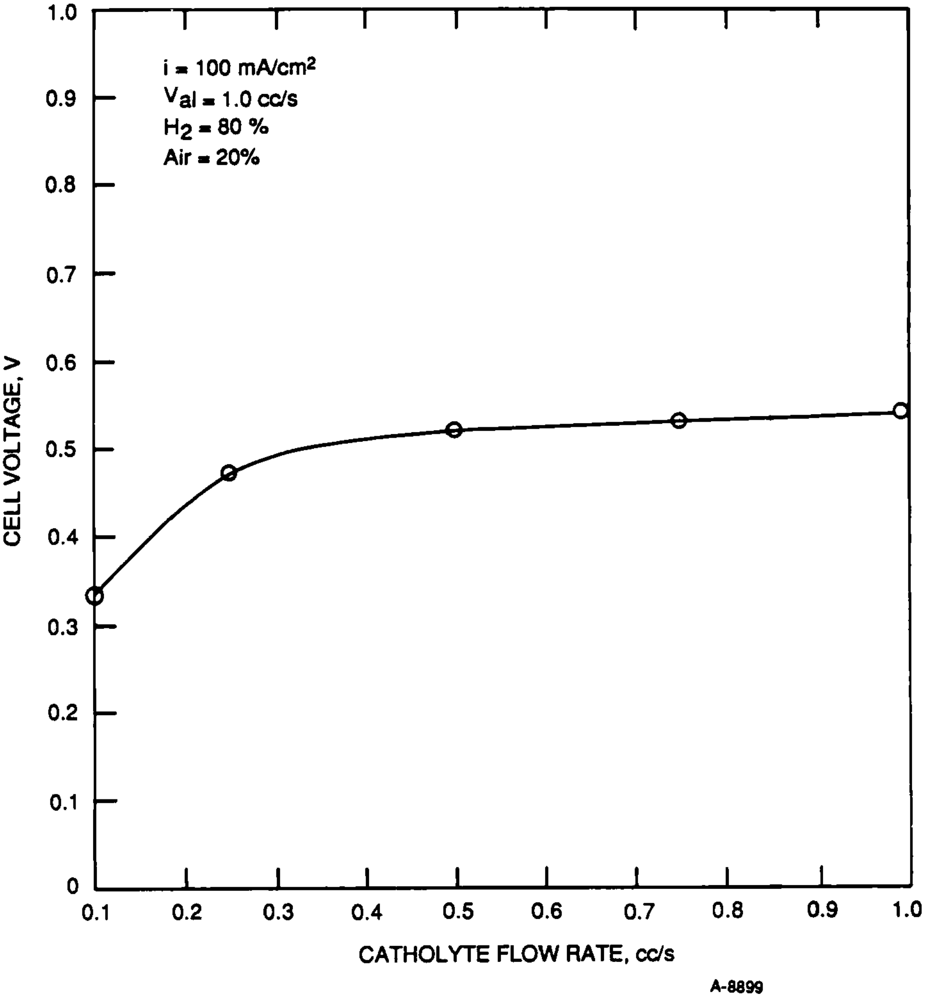

FIG. 8. Effect of catholyte flow rate on the ECC cell voltage.

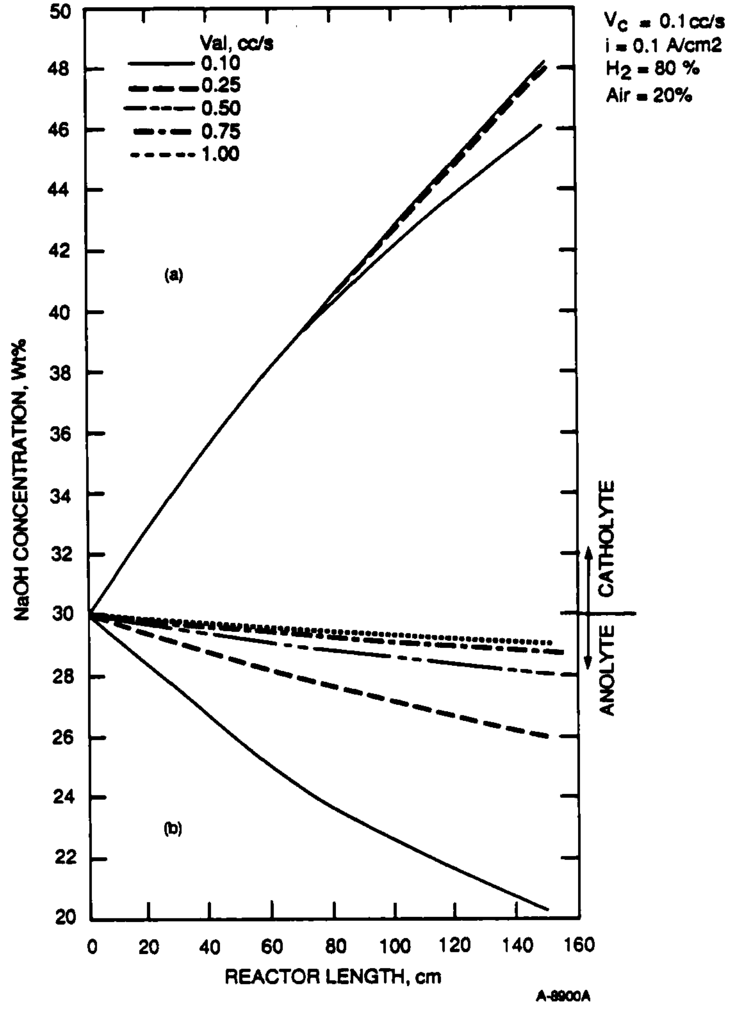

FIG. 9. Effect of anolyte flow rate on (a) catholyte concentration profile and (b) anolyte concentration profile in the ECC.

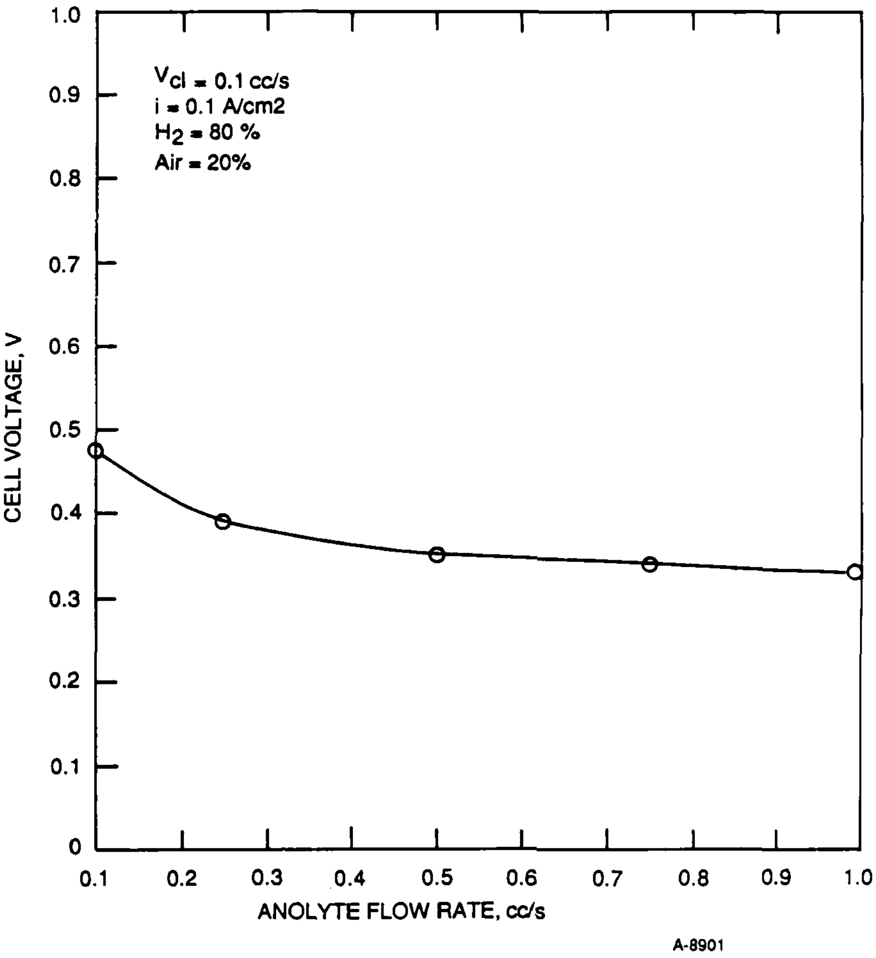

FIG. 10. Effect of anolyte flow rate on the ECC cell voltage.

The effect of the anolyte flow rate on the resulting ECC cell voltage is shown in Figs. 10. Contrary to the effect observed on the effect of catholyte flow rate, the cell voltage initially decreased noticeably as the anolyte flow rate was increased from 0.1 to 0.25 cm^3/s and remained relatively unchanged for higher anolyte flow rates. The higher cell voltages observed at lower flow rates are due to decreasing membrane and electrolyte resistances as the anolyte concentration decreases.

The process of concentrating the dilute inlet caustic solution can be achieved by either 1) removing water at the cathode electrochemically, 2) adding concentrated caustic across the membrane from the anolyte compartment, or 3) a combination of these two processes. Consequently, we investigated the effect of different membranes with different transport and conductivity properties on the ECC performance. Three different membranes were chosen for the study. They include: 1) Du Pont's A-1 membrane, 2) RAI's R-5010 membrane, and 3) RAI's R-1010 membrane. The catholyte flow rate was set at 0.1 cm^3/s and the anolyte flow rate was set at 1.0 cm^3/s. In Fig. 11(a) we present the catholyte concentration profiles for the three different membranes. Membranes A-1 and R-5010 perform equally well in concentrating the caustic whereas Membrane R-1010 performs comparatively poorer than the other two membranes. An interesting feature to note is that although Membrane A-1 with a high sodium transport number initially performs better than Membrane R-5010 with a low sodium transport number, the exit concentration with R-5010 becomes higher than with A-1. This is because A-1 ends up transporting more water than R-5010, making it relatively less efficient in concentrating the caustic. Membrane R-1010 continuously performs poorer because it not only has a poor sodium transport number but also a high water transport number. Thus these simulations predict that cation-exchange membranes with high sodium selectivity are not a necessary condition for use in the ECC.

The cell voltage data for the different membranes are shown in Fig. 12. The cell voltages with R-5010 and R-1010 are much higher than those obtained with A-1. For example, the cell voltage with R-1010 is almost twice as high as with Membrane A-1. This implies that the ECC with the RAI membranes will deliver more power than the A-1 membrane. The cell voltage increases in the order of A1 → R-5010 → R-1010 due to increasing membrane conductivity in the same order.

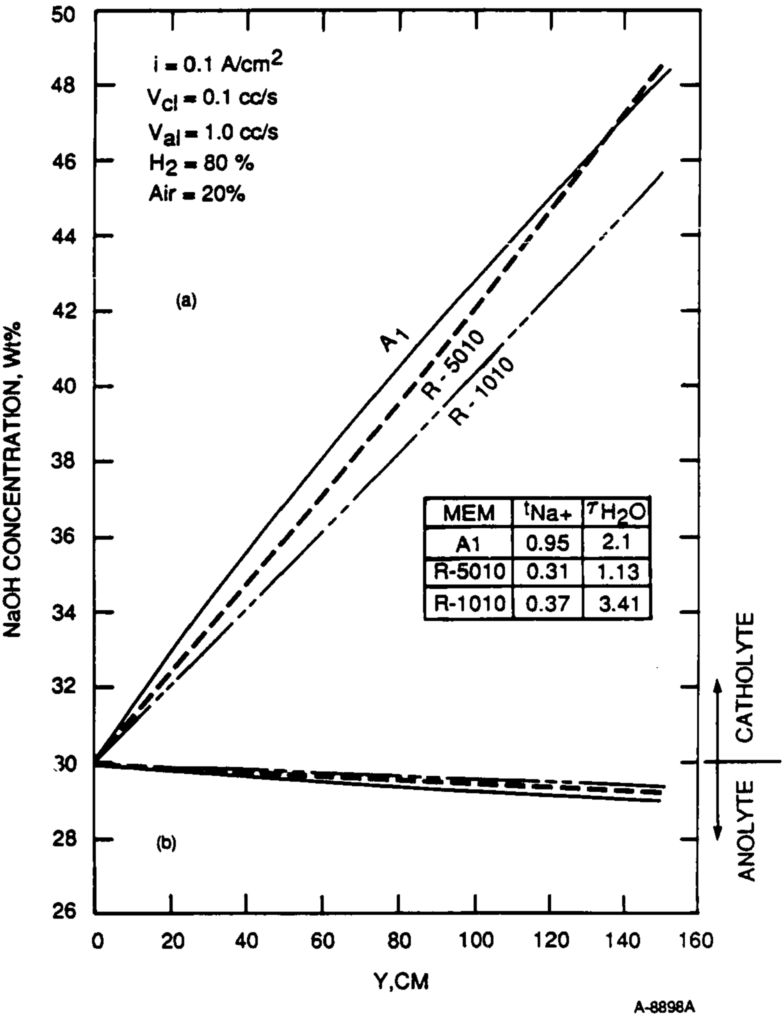

MEM	t_{Na+}	τ_{H_2O}
A1	0.95	2.1
R-5010	0.31	1.13
R-1010	0.37	3.41

FIG. 11. Effect of membranes on (a) catholyte concentation profile and (b) anolyte concentration profile in the ECC.

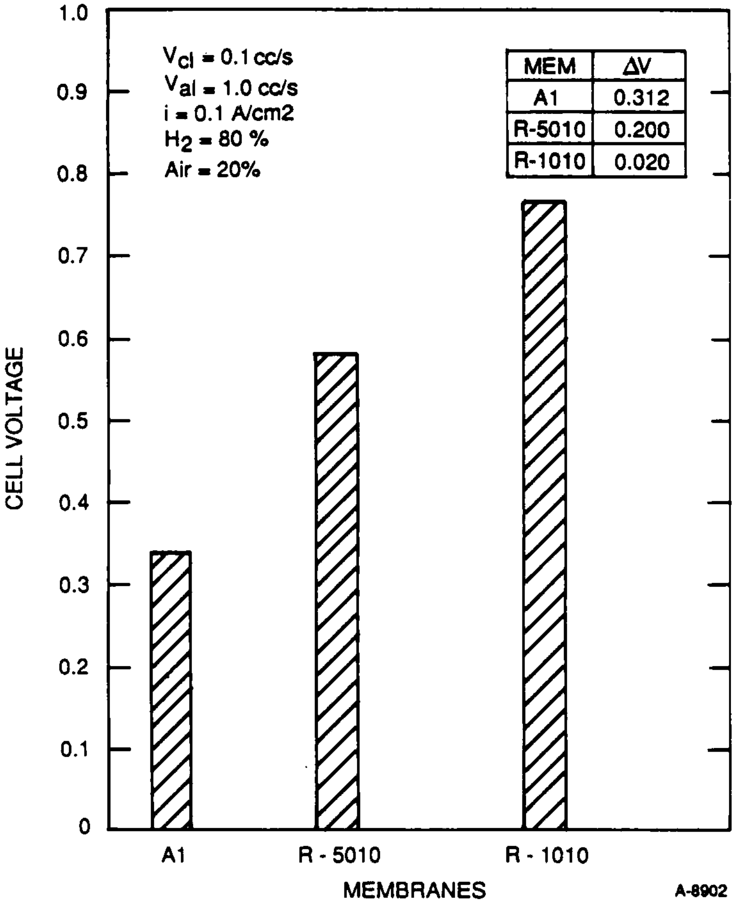

MEM	ΔV
A1	0.312
R-5010	0.200
R-1010	0.020

FIG. 12. Effect of membranes on the ECC cell voltage.

SUMMARY

In summary, it was found possible to concentrate a 30 wt% dilute caustic feed stream to 50 wt% and also simultaneously generate dc electricity using the PSI electrochemical caustic concentrator. The anolyte and catholyte flow rates are important process parameters and determine the concentration profile and the exit concentration of the caustic in the ECC. In general, the lower the electrolyte flow rate, the higher the exit catholyte concentration and the lower the anolyte concentration. The resulting cell voltage is a function of the concentration profiles in the anolyte and the catholyte. The cell voltage increases with decreasing anolyte concentrations and decreases with increasing catholyte concentrations. Moreover, analysis with different membranes suggests that high sodium selectivity is not the most important criterion for selection of a membrane for the ECC. Rather, the total water transported across the membrane from the anolyte is most important. For example, if the relative water transport is 3, then a membrane with a sodium transport of 0.9 brings in three times as much water per Faraday as a membrane with a sodium transport number of 0.3! Consequently, membranes like the R-5010 or R-1010 with low sodium transport number are more attractive for use in the ECC. Furthermore, these membranes generally have higher conductivities and consequently are capable of delivering higher cell voltages. In the future we will evaluate Du Pont's NAFION 117 due to its excellent conductivity in caustic electrolyte. (NAFION is a registered trademark of the E. I. du Pont de Nemours and Co.)

Acknowledgments

The authors acknowledge the financial support of the DOE under Cooperative agreement No. DEFC07-845D12495. Helpful discussions with Mr. W. Sonnett and Dr. S. Priebee of DOE are appreciated. Additionally, we acknowledge Du Pont for supplying developmental cation-exchange membranes for this program. Also, we acknowledge valuable discussions with Dr. L. Bu:ton and Mr. D. Brandt of Du Pont. Finally, we acknowledge electrocatalyst and electrode development efforts of Mr. G. Moniz and E. Anderson and Ms. M. Clawson of PSI.

REFERENCES

1. N. P. Yao, in *Proceedings of the Workshop on Energy Conservation in Industrial Electrochemical Processes,* ANL/OEPM-77, Contract W-31-109-Eng-38; Argonne National Laboratory, Argonne, Illinois, 1976.
2. D. E. Hall and E. Spore, *J. Electrochem. Soc., 132*(7), 252C–285C (1985).
3. A. Gelb "Process for Generating Chlorine and Caustic Soda Using a Membrane Electrolysis Cell Coupled to a Membrane Alkaline Fuel Cell," U.S. Patent 4,647,351 (March 3, 1987).
4. A. Gelb and E. J. Taylor, *Application of Fuel Cells to Chlorine-Caustic Technology,* AIChE Symposium Series, No. 250, Volume 82, 1986.
5. E. J. Taylor, G. Moniz, M. Clawson, E. Anderson, and G. Wilemski, "Development of Porous Gas Diffusion Electrodes for Oxygen Reduction in Alkaline Media," *Extended Abstracts, Electrochemical Society Meeting,* Chicago, October 9–14, 1988.
6. E. J. Taylor, N. R. K. Vilambi, R. Waterhouse, and A. Gelb, "Transport and Conductivity Properties of Cation Exchange Membranes in Concentrated Caustic Solution," *J. Membr. Sci.,* Submitted for Publication.
7. E. J. Taylor, A. Gelb, and J. Campbell, *Application of Fuel Cells to Chlorine-Caustic Technology,* DOE Technical Report, DOE Contract No. DEFc07-845D12495.
8. R. H. Perry and C. H. Chilton, *Chemical Engineers Handbook,* 5th ed., McGraw-Hill, New York, p. 3–45.
9. E. W. Washburn, (Editor in Chief), *International Critical Tables of Numerical Data, Physics, Chemistry and Technology,* Vol. III, McGraw-Hill, New York, 1928, p. 79.

Received by editor May 24, 1989